The Plant Cell, Vol. 26: 3036–3050, July 2014, www.plantcell.org

Combined Increases in Mitochondrial Cooperation and Oxygen Photoreduction Compensate for Deficiency in Cyclic Electron Flow in *Chlamydomonas reinhardtii*[W][OPEN]

Kieu-Van Dang,[a,b,c,1] Julie Plet,[a,b,c,1] Dimitri Tolleter,[a,b,c,2] Martina Jokel,[d] Stéphan Cuiné,[a,b,c] Patrick Carrier,[a,b,c] Pascaline Auroy,[a,b,c] Pierre Richaud,[a,b,c] Xenie Johnson,[a,b,c] Jean Alric,[a,b,c] Yagut Allahverdiyeva,[d] and Gilles Peltier[a,b,c,3]

[a] CEA, Institut de Biologie Environnementale et de Biotechnologie, Laboratoire de Bioénergétique et Biotechnologie des Bactéries et Microalgues, CEA Cadarache, F-13108 Saint-Paul-lez-Durance, France
[b] CNRS, UMR 7265 Biologie Végétale et Microbiologie Environnementale, F-13108 Saint-Paul-lez-Durance, France
[c] Aix Marseille Université, UMR 7265 Biologie Végétale et Microbiologie Environnementale, F-13284 Marseille, France
[d] Laboratory of Molecular Plant Biology, Department of Biochemistry, University of Turku, FI-20014 Turku, Finland

During oxygenic photosynthesis, metabolic reactions of CO_2 fixation require more ATP than is supplied by the linear electron flow operating from photosystem II to photosystem I (PSI). Different mechanisms, such as cyclic electron flow (CEF) around PSI, have been proposed to participate in reequilibrating the ATP/NADPH balance. To determine the contribution of CEF to microalgal biomass productivity, here, we studied photosynthesis and growth performances of a knockout *Chlamydomonas reinhardtii* mutant (*pgrl1*) deficient in PROTON GRADIENT REGULATION LIKE1 (PGRL1)–mediated CEF. Steady state biomass productivity of the *pgrl1* mutant, measured in photobioreactors operated as turbidostats, was similar to its wild-type progenitor under a wide range of illumination and CO_2 concentrations. Several changes were observed in *pgrl1*, including higher sensitivity of photosynthesis to mitochondrial inhibitors, increased light-dependent O_2 uptake, and increased amounts of flavodiiron (FLV) proteins. We conclude that a combination of mitochondrial cooperation and oxygen photoreduction downstream of PSI (Mehler reactions) supplies extra ATP for photosynthesis in the *pgrl1* mutant, resulting in normal biomass productivity under steady state conditions. The lower biomass productivity observed in the *pgrl1* mutant in fluctuating light is attributed to an inability of compensation mechanisms to respond to a rapid increase in ATP demand.

INTRODUCTION

Oxygenic photosynthesis is a highly integrated bioenergetic and metabolic process that converts solar energy into chemical energy in land plants, microalgae, and cyanobacteria. During oxygenic photosynthesis, electron transfer reactions operating within thylakoid membranes generate both reducing (NADPH) and phosphorylating (ATP) powers, subsequently used to fuel metabolic reactions of CO_2 fixation in the chloroplast stroma. In natural conditions, photosynthetic organisms face constant environmental changes (illumination, temperature, availability of nutrients, and water, etc.), which may differentially affect the efficiency of electron transfer and metabolic reactions, possibly resulting in imbalances between the production and use of chemical energy. Any disequilibrium between energy supply and demand can damage photosynthetic cells since it can lead to overreduction of photosynthetic electron acceptors and to the generation of reactive oxygen species and finally to photooxidative stress. To avoid negative effects of environmental fluctuations, photosynthetic organisms have developed a set of cellular mechanisms allowing them to fine-tune the supply of energy to the demand (Asada, 1999; Niyogi, 2000; Peers et al., 2009; Peltier et al., 2010).

A key parameter for optimal functioning of photosynthesis is the balance between reducing power (NADPH) and phosphorylating power (ATP). It is generally considered that the reactions of linear electron transfer, which involve both photosystem II (PSII) and photosystem I (PSI) operating in series, generate less ATP than is required for the metabolic reactions of photosynthesis (Osmond, 1981; Kramer and Evans, 2011; Foyer et al., 2012). Moreover, the ATP demand varies depending on the environmental conditions and on the metabolic status. In land plants, the ATP demand increases under high light and CO_2 limitation due to the activity of photorespiration (Osmond, 1981; Munekage et al., 2008). In addition, when exposed to low CO_2 concentration, microalgae and cyanobacteria induce a CO_2-concentrating mechanism (CCM), which requires extra ATP (Karlsson et al., 1994; Fridlyand, 1997; Duanmu et al., 2009; Lucker and Kramer, 2013).

Different mechanisms have been proposed to be responsible for reequilibration of the NADPH/ATP balance and avoiding

[1] These authors contributed equally to this work.
[2] Current address: Division of Plant Science, Research School of Biology, The Australian National University, Canberra, ACT, Australia.
[3] Address correspondence to gilles.peltier@cea.fr.
The author responsible for distribution of materials integral to the findings presented in this article in accordance with the policy described in the Instructions for Authors (www.plantcell.org) is: Gilles Peltier (gilles.peltier@cea.fr).
[W] Online version contains Web-only data.
[OPEN] Articles can be viewed online without a subscription.
www.plantcell.org/cgi/doi/10.1105/tpc.114.126375

overreduction of the NADPH stromal pool and of photosynthetic electron acceptors (Kramer and Evans, 2011). The most studied is cyclic electron flow (CEF), which generates extra proton gradient by recycling electrons around PSI, thus resulting in the supply of extra ATP. This CEF pathway, described as antimycin A sensitive, involves ferredoxin (Fd), PROTON GRADIENT REGULATION5 (Munekage et al., 2002), and PROTON GRADIENT REGULATION LIKE1 (PGRL1) proteins (DalCorso et al., 2008; Iwai et al., 2010), the latter was recently proposed to act as a Fd-quinone reductase enzyme (Hertle et al., 2013). Another CEF pathway, described as antimycin A insensitive, operates in thylakoid membranes of land plants (Joët et al., 2001; Munekage et al., 2002) and microalgae (Ravenel et al., 1994). The latter involves the multiple-subunit NADH dehydrogenase complex (NDH-1) of land plant chloroplasts (Joët et al., 2001; Munekage et al., 2004; Rumeau et al., 2005). The plastidial NDH-1 complex is absent from microalgal species, where a plastidial type II NAD(P)H dehydrogenase (NDA2) catalyzing plastoquinone (PQ) reduction has been suggested to participate in CEF (Jans et al., 2008; Desplats et al., 2009; Peltier et al., 2010).

Mitochondrial respiration may also participate in the reequilibration between the reducing and phosphorylating power within the cell. This has been experimentally supported by the effect of respiratory inhibitors on photosynthesis (Krömer and Heldt, 1991; Krömer, 1995) or by the study of mutants affected in plastidial ATPase (Lemaire et al., 1988) or in mitochondrial respiration (Cardol et al., 2009). Metabolic shuttles such as the malate-oxaloacetate shuttle would export reducing power from the chloroplast toward the cytosol and subsequently from the cytosol to the mitochondria (Scheibe, 2004; Shen et al., 2006). Oxygen photoreduction at PSI, also called Mehler reactions, has long been proposed to supply extra ATP for photosynthesis through pseudocyclic photophosphorylations (Allen, 1975). Although Mehler reactions were widely studied in the 1970s, mostly using thylakoid preparations, their contribution in vivo is less clear (Kramer and Evans, 2011). The recent discovery of flavodiiron (FLV) proteins in cyanobacteria provided evidence at the molecular level for the existence of special types of oxygen photoreduction processes downstream of PSI (Helman et al., 2003; Allahverdiyeva et al., 2013). However, Mehler reactions and Mehler-like reactions driven by FLVs are different processes, the former generating reactive oxygen species (ROS) (Asada, 1999), but the latter not (Vicente et al., 2002; Helman et al., 2003). While *FLV* genes showing high homology with cyanobacterial genes are present in microalgae genomes (Peltier et al., 2010), their physiological significance and their possible involvement in Mehler-like reactions remain to be established.

From the screening of an insertional mutant library based on the analysis of chlorophyll fluorescence transients, we recently isolated a *Chlamydomonas reinhardtii* knockout mutant of the *PGRL1* gene. The *pgrl1* mutant showed decreased activity of CEF and increased capacity to produce hydrogen under anaerobic conditions (Tolleter et al., 2011). In this work, we investigated physiological adaptations occurring under aerobic conditions in response to the impairment of PGRL1-mediated cyclic electron flow. Based on biomass productivity measurements and on the analysis of different photosynthetic parameters in cells grown under different light regimes and CO_2 concentrations, we conclude that under a wide range of environmental conditions, deficiency in CEF is compensated for by the concerted action of different mechanisms, including mitochondrial respiration and oxygen photoreduction, resulting in normal steady state growth. Growth retardation in the mutant was observed only in conditions of high ATP demand (low CO_2) and fluctuating illumination. While dispensable in steady state growth conditions, PGRL1-mediated CEF would confer a selective advantage in response to rapid changes in the environment.

RESULTS

Photosynthetic Properties of *pgrl1* Grown Photoautotrophically under Various CO_2 and Light Regimes

Photosynthetic activities of the *pgrl1* mutant and its wild-type progenitor were measured by means of chlorophyll fluorescence in cells grown photoautotrophically in different conditions by changing CO_2 supply (either 0.04% CO_2 for "air" or 2% CO_2 in air for "CO_2") and light intensity (50 μmol photons m^{-2} s^{-1} for low light [LL] and 200 μmol photons m^{-2} s^{-1} for high light [HL]). The use of a pulse-modulated amplitude fluorometer enabled the determination of both photosynthetic electron transport rate (ETR; Figures 1A to 1D) and nonphotochemical quenching (NPQ; Figures 1E to 1H). Under most growth conditions ("CO_2 LL," "air LL," and "CO_2 HL"), the ETR of *pgrl1* was slightly higher than that of the wild-type progenitor line (Figures 1A to 1C). Under "air HL" conditions, ETR was diminished in the wild-type line compared with "air LL" conditions, the decrease being much more pronounced in *pgrl1* (Figure 1D). The ETR decrease observed in "air HL"-grown *pgrl1* cells resulted from a decrease in the PSII yield and an increase in the electron pressure on the PSII acceptor Q_A monitored by the 1-qP parameter (Supplemental Figures 1A and 1B). A decrease in the maximal photochemical PSII yield (measured as *Fv*/*Fm* after 30 min dark adaptation) was also observed in "air HL" in *pgrl1* but not in the wild type (Supplemental Figures 1C and 1D). Under most growth conditions ("CO_2 LL," "air LL," and "CO_2 HL"), NPQ was slightly lower in *pgrl1* than in the wild-type line (Figures 1E to 1G). This effect was previously attributed to a decrease in qE resulting from a lower pH gradient in the mutant in the absence of PGRL1-mediated CEF (Tolleter et al., 2011). Surprisingly, NPQ was strongly increased in *pgrl1* under "air HL" compared with the wild-type progenitor (Figure 1H).

Transition to State 2 Is Triggered in *pgrl1* under High Light and Low CO_2

To determine whether the NPQ increase might result from another component of NPQ, such as state transition (qT), we performed low temperature (77K) chlorophyll fluorescence emission measurements in light-adapted algal samples (Figures 2A and 2B). Under "CO_2 HL" conditions, fluorescence spectra of *pgrl1* and wild-type lines were similar (Figures 2A and 2C). When cells were grown in "air HL" conditions, a large increase of the 710-nm fluorescence peak was observed in *pgrl1* (Figures 2B and 2C). Such an increase in the 710-nm fluorescence peak

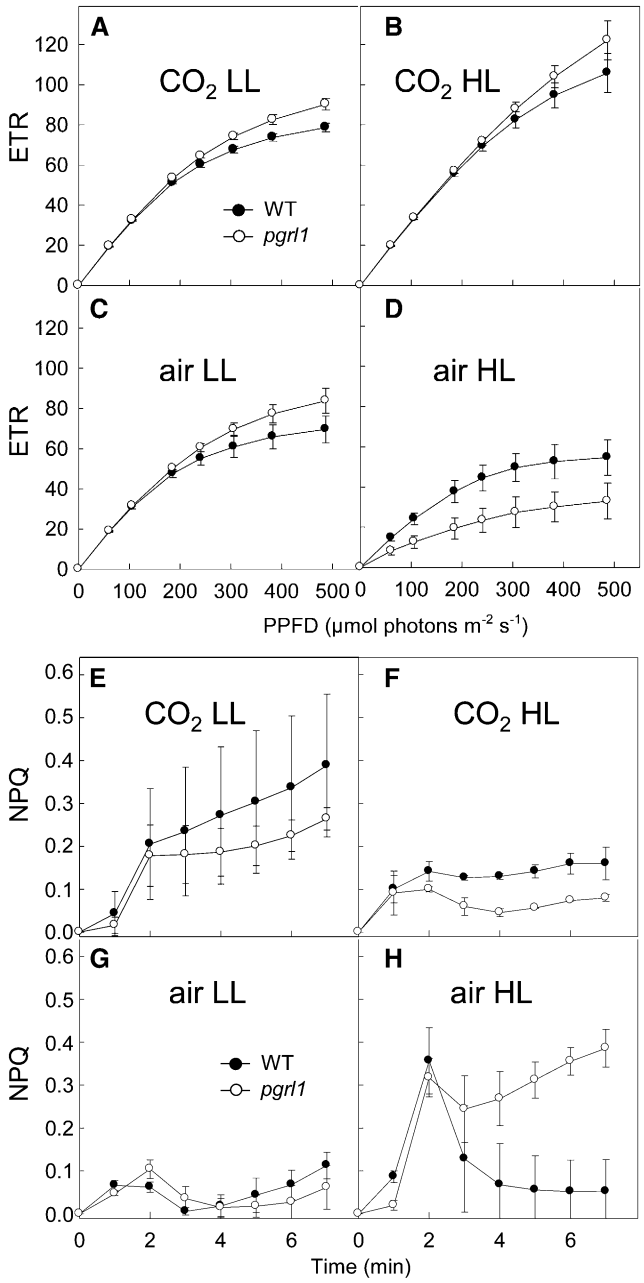

Figure 1. ETR and NPQ Measured in Wild-Type and *pgrl1 C. reinhardtii* Lines Grown Photoautotrophically under Two Different Light Intensities and CO_2 Concentrations.

ETR (**[A]** to **[D]**) and NPQ (**[E]** to **[H]**) were determined from pulse-modulated chlorophyll fluorescence measurements. Cells (2.5×10^6 cells mL^{-1}) were sampled during exponential growth of batch cultures. Cells were grown in LL (**[A]**, **[C]**, **[E]**, and **[G]**) (50 μmol photons m^{-2} s^{-1}), HL (**[B]**, **[D]**, **[F]**, and **[H]**) (200 μmol photons m^{-2} s^{-1}), 2% CO_2-enriched air (**[A]**, **[B]**, **[E]**, and **[F]**), and air (**[C]**, **[D]**, **[G]**, and **[H]**). Wild-type progenitor line (closed circles); *pgrl1* mutant (open circles). Shown are means ± SD (n = 3).

indicates that light harvesting complex II (LHCII) is more connected to PSI than to PSII as it is the case in State 2 in response to the phosphorylation of LHCII (Wollman and Delepelaire, 1984). To test this interpretation, we performed immunodetection of phosphorylated LHCII proteins using an antiphosphothreonine antibody (Figures 2D and 2E). When *C. reinhardtii* cells are in State 2, LHCII proteins CP29, CP26, and LHCP11 are phosphorylated (Fleischmann et al., 1999). A higher level of phosphorylation of LHCII proteins was observed in *pgrl1* compared with its wild-type progenitor when cells were grown in "air HL" (Figures 2D and 2E). However, since the 710-nm emission fluorescence peak observed in the mutant is much stronger than previously reported in response to physiological situations (Takahashi et al., 2013), it is likely that the large increase in the 710-nm peak does not solely result from state transition, but also from a decrease in PSI (Delepelaire and Wollman, 1985). This question is addressed below.

Biomass Productivity of *pgrl1* Is Not Affected under Constant Light, but Reduced under Fluctuating Light

To determine growth properties of the *pgrl1* mutant and its wild-type progenitor in different conditions of CO_2 supply and illumination, cells were cultivated in 1-liter photobioreactors operated as turbidostats. In this experimental setup, the cell density of the culture was measured by an OD probe and maintained constant by addition of fresh medium. We first determined, in this new setup, light conditions leading to similar effects as previously observed in the flask cultures (Figure 1). LL and HL incident illuminations were increased from 50 to 120 μmol photons m^{-2} s^{-1} (LL) and from 200 to 500 μmol photons m^{-2} s^{-1} (HL), respectively, to take into account differences in light paths between these two setups. Two parameters were determined, ETR capacity (measured at 400 μmol photons m^{-2} s^{-1}) and the 77K chlorophyll fluorescence emission peak ratio E_{685}/E_{710} (Supplemental Figure 2). In the presence of high CO_2, no difference was noticed between ETR capacities of *pgrl1* and wild-type lines, ETR progressively increasing for both strains as the growth irradiance rose (Supplemental Figure 2A). In these conditions, no major change in the fluorescence E_{685}/E_{710} emission peak ratio was observed, except transiently when switching from 360 to 500 μmol photons m^{-2} s^{-1} (Supplemental Figure 2C). In the presence of air CO_2 levels, both ETR and E_{685}/E_{710} ratio remained mostly constant in the wild-type line, but progressively decreased in *pgrl1* as the light intensity increased (Supplemental Figures 2B and 2D). The decrease in ETR was maximal at 500 μmol photons m^{-2} s^{-1} with full ETR activity reestablished after 1 h at 120 μmol photons m^{-2} s^{-1} (LL); a return to the initial the E_{685}/E_{710} ratio was observed after 24 h. We conclude from this experiment that the changes in photosynthetic parameters observed in the *pgrl1* mutant when grown in "air HL" conditions are reversible.

Specific growth rates were determined from the measurement of fresh culture medium added to the turbidostat to maintain a constant biomass concentration (Figures 3A and 3B). The growth rate measured under "CO_2 HL" (~3 d^{-1}) was higher than under "CO_2 LL" (~1 d^{-1}), but no significant growth difference was observed between *pgrl1* and wild-type lines (Figure 3A).

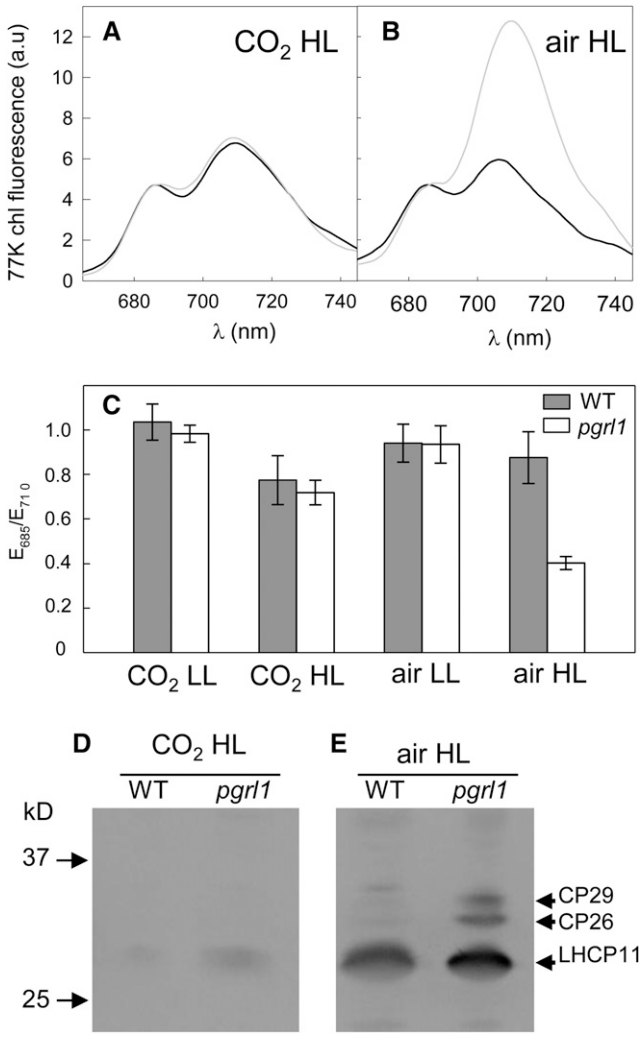

Figure 2. State Transition Analyzed by Low Temperature (77K) Emission Spectra of Chlorophyll Fluorescence and LHCII Phosphorylation in Wild-Type and *pgrl1* Mutant *C. reinhardtii* Lines.

Cells were grown photoautotrophically in batch cultures under 200 μmol photons m^{-2} s^{-1} (HL; **[A]** to **[E]**) or 50 μmol photons m^{-2} s^{-1} (LL; **[C]**) in 2% CO_2-enriched air (**[A]**, **[C]**, and **[D]**) or air (**[B]**, **[C]**, and **[E]**). Samples were loaded at equal protein amounts based on Coomassie blue staining. LHCII proteins CP29, CP26, and LHCP11, which are phosphorylated in State 2 conditions but not in State 1, are shown (Fleischmann et al., 1999).
(A) and **(B)** 77K chlorophyll fluorescence emission spectra; wild-type progenitor line (black line); *pgrl1* cells (gray line).
(C) E_{685}/E_{710} chlorophyll fluorescence emission ratios measured in light-adapted *pgrl1* (white bars) and wild-type (dark bars) lines grown under different light intensities and CO_2 concentrations.
(D) and **(E)** Immunodetection of phosphorylated LHCII using an anti-phosphothreonine antibody in light-adapted *pgrl1* and wild-type cells grown in HL in the presence of 2% CO_2-enriched air **(D)** or in the presence of air **(E)**.

Under air conditions, no difference in growth rates was observed between LL- and HL-grown cells (Figure 3B), showing that growth is limited by CO_2 availability. Again, no growth difference was observed between wild-type and *pgrl1* lines, despite a decrease in the maximal photosynthetic capacity of the mutant (measured by chlorophyll fluorescence parameters at saturating CO_2; see Figure 1). Growth performances were also assayed on a solid medium by plating serial dilutions of a liquid culture onto Petri dishes (Figures 3C and 3D). While no difference was observed between wild-type and mutant strains under low light (50 μmol photons m^{-2} s^{-1}), growth was strongly reduced in *pgrl1* at high light (200 μmol photons m^{-2} s^{-1}), but only in the presence of low CO_2 (air) levels (Figures 3C and 3D). Such a difference in growth performances observed between liquid and solid cultures was quite surprising. It may result from differences in physiological situations experienced by cells in the two modes of cultivation. In liquid cultures, cells were grown under steady state conditions. For the solid tests, cells were plated onto a solid medium from liquid cultures, therefore experiencing a strong change in light intensity. In order to test this hypothesis, low-density liquid cultures (4×10^5 cells mL^{-1}) were adapted to 50 μmol photons m^{-2} s^{-1} for 48 h and then submitted to a sudden light increase to 800 μmol photons m^{-2} s^{-1}. Dilution with fresh medium was stopped in order to measure as accurately as possible the biomass increase during the transient (Figures 3E to 3H). At high CO_2 levels, the initial OD increase observed in response to HL was faster in *pgrl1* than in its wild-type progenitor line, but then resumed at a similar rate (Figures 3E and 3G). Under air, severe growth retardation was observed in the mutant compared with the wild-type line (Figures 3F and 3H). This suggests that growth differences observed on a solid medium are the result of a higher sensitivity of the *pgrl1* mutant to a LL to HL transient.

To further determine the effect of HL pulses on growth, specific growth rates were measured at 50 μmol photon m^{-2} s^{-1} and in the presence of an additional 1-min HL pulse (50/800 μmol photon m^{-2} s^{-1} 5/1 min) as recently studied in the *Arabidopsis thaliana pgr5* mutant (Suorsa et al., 2012). In the presence of high CO_2 levels, both mutant and wild-type strains gained from the additional light supplied by the high light pulse by increasing their specific growth rates (Figure 3I). In the presence of low CO_2 levels (air), only the wild-type line could take advantage of the additional light pulse, the specific growth rate of the mutant remaining unchanged (Figure 3J). We conclude from these experiments that PGRL1-dependent CEF is not essential for steady state growth under a wide range of CO_2 levels and light intensities but is important when HL transients are experienced at low CO_2 concentration.

pgrl1 Photosynthesis Is More Dependent on Mitochondrial Respiration

The similar growth performances observed at steady state for both *pgrl1* and wild-type lines under a wide range of environmental conditions, strongly suggest the involvement of mechanisms that compensate for ATP deficiency due to the impairment in PGRL1-mediated CEF. In the wild-type, PGRL1 amounts were higher at HL than at LL (at high CO_2) and higher at low CO_2 than at high CO_2 (at HL), indicating an increased contribution of CEF in these conditions (Supplemental Figure 3). We observed no increase in NDA2 amounts either in the wild type or in *pgrl1* (Supplemental Figure 3), indicating that no compensation occurred via upregulation of NDA2 in these conditions. We then

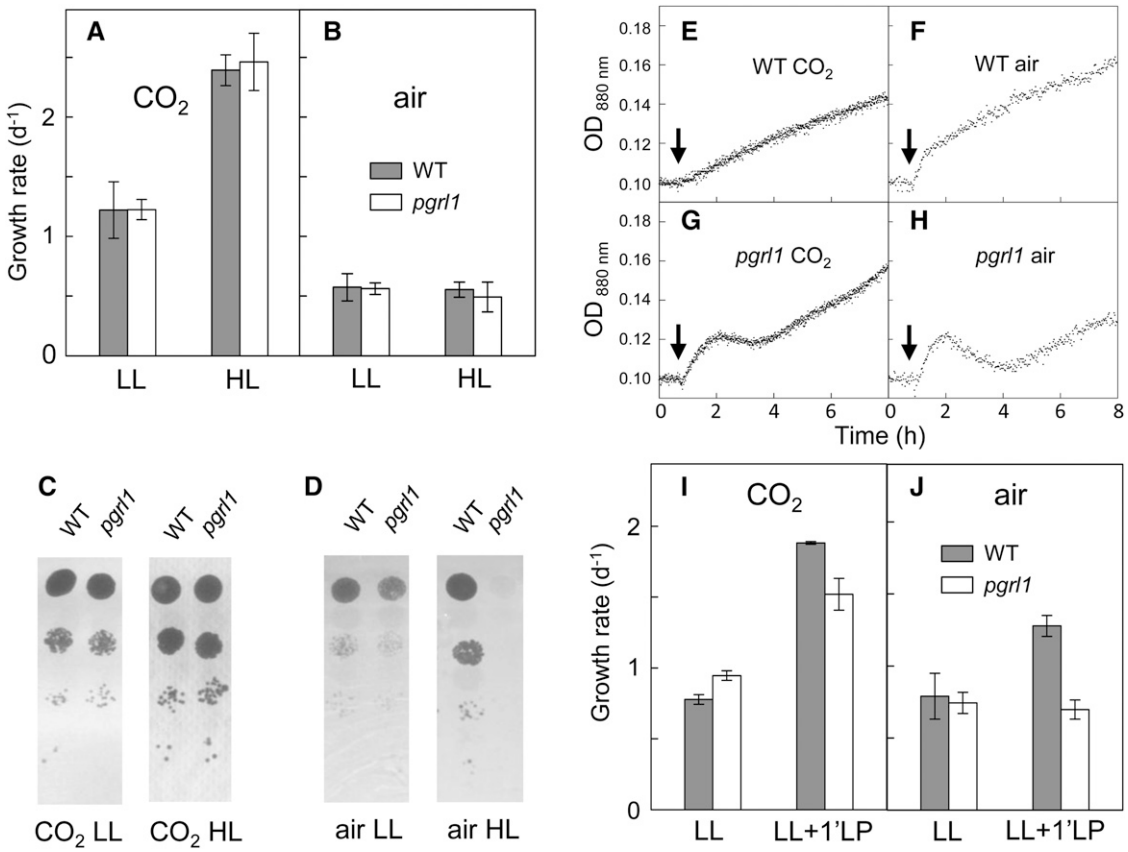

Figure 3. Growth Performances of *pgrl1* and Wild-Type *C. reinhardtii* Lines Cultivated Photoautotrophically in Liquid or Solid Media.

(A) and **(B)** Growth performances were analyzed in liquid cultures using 1-liter photobioreactors operated as turbidostats. Cell density was measured using an absorption probe and maintained at a constant level (≈1.5 × 10^6 cells mL^{-1}) by injection of fresh medium. Growth rates were measured in LL (120 μmol photons m^{-2} s^{-1}) or HL (500 μmol photons m^{-2} s^{-1}) in cells grown in the presence of 2% CO_2-enriched air **(A)** or air **(B)**. Wild-type progenitor line (dark bars); *pgrl1* mutant (white bars). Shown are means ± SD (n = 7 in **[A]** or n = 3 in **[B]**).

(C) and **(D)** Growth on solid medium was assessed by plating serial (1/10) dilutions of an algal culture (initial culture concentration 10^6 cells mL^{-1}) on a minimal medium under constant LL (50 μmol photons m^{-2} s^{-1}) or HL (200 μmol photons m^{-2} s^{-1}) in the presence of air enriched with 2% CO_2 **(C)** or air **(D)**. Shown are representative cultures out of three biological repeats showing similar effects.

(E) to **(H)** Growth performances of *pgrl1* and the wild type in response to LL to HL switch. The culture was maintained at a low cell density (≈4 × 10^5 cells mL^{-1}) by injection of fresh medium during a 48-h period at 50 μmol photons m^{-2} s^{-1}. When indicated by arrows, light intensity was increased to 800 μmol photons m^{-2} s^{-1}. The injection of fresh medium was stopped and the OD_{880} increase recorded. Wild-type line (**[E]** and **[F]**); *pgrl1* (**[G]** and **[H]**). Transients shown are representative of three independent experiments.

(I) and **(J)** Growth performances of *pgrl1* and wild-type lines under fluctuating light. Low cell density (≈4 × 10^5 cells mL^{-1}) cultures were performed at 50 μmol photons m^{-2} s^{-1} (LL) or under a 50/800 μmol photons m^{-2} s^{-1} (5 min/1 min) fluctuating light regime (LL+1'LP). Wild-type progenitor line (dark bars) and *pgrl1* (white bars). Shown are means ± SD (n = 2).

evaluated to what extent increased cooperation with mitochondrial respiration might contribute. For this purpose, the effect of respiratory inhibitors was assessed on photosynthetic activities (Figure 4). In *C. reinhardtii*, simultaneous addition of inhibitors of cytochrome *bc* and of the alternative respiration pathway is required to fully inhibit the respiratory chain (Cournac et al., 2002). When salicyl hydroxamic acid (SHAM), an inhibitor of the alternative oxidase was added, no significant change in chlorophyll fluorescence was observed. When myxothiazol, an inhibitor of the mitochondrial cytochrome bc_1 complex, was subsequently added, an increase in the stationary fluorescence level (*Fs*) was observed in *pgrl1* but not in its wild-type progenitor line (Figure 4A), resulting in a drop in the PSII yield (Figures 4D and 4E). Quenching analysis revealed a strong increase of the 1-qP parameter in the mutant after treatment with respiratory inhibitors, indicating a higher reduction of PSII electron acceptors (Figures 4B and 4C). The effect was even more pronounced in *pgrl1* mutant cells grown in air (Figures 4C and 4E). We conclude from this experiment that photosynthetic activity of the *pgrl1* mutant is more dependent on cooperation with mitochondrial respiration than is that of its wild-type progenitor line, the cooperation being increased in conditions (such as low CO_2) where the ATP demand is increased.

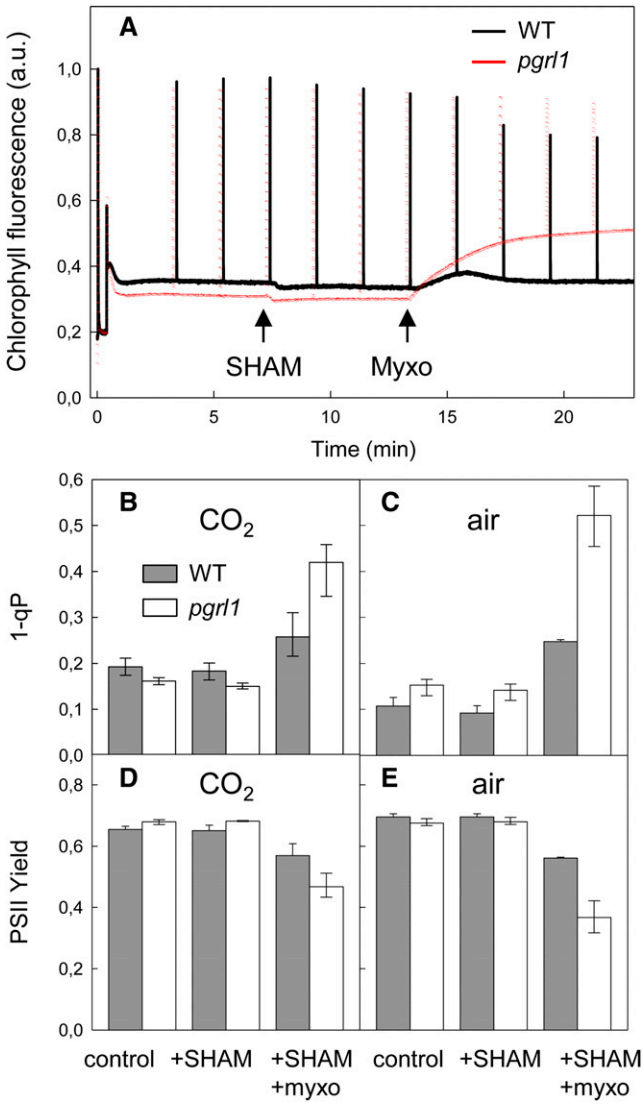

Figure 4. Effect of Respiratory Inhibitors on Photosynthetic Activity of *C. reinhardtii* Wild-Type and *pgrl1* Lines Measured by Chlorophyll Fluorescence.

(A) Wild-type progenitor (black) and *pgrl1* (red) lines were grown photoautotrophically in 1-liter photobioreactors operated as turbidostats at a constant biomass concentration (≈1.5 × 10^6 cells mL^{-1}) at a light intensity of 120 μmol photons m^{-2} s^{-1} in the presence air enriched with 2% CO_2. Chlorophyll fluorescence measurements were performed under a light intensity of 150 μmol photons m^{-2} s^{-1} in the presence of 5 mM $NaHCO_3$. When indicated by arrows, respiratory inhibitors SHAM and myxothiazol were sequentially added at respective concentrations of 0.4 mM and 2 μM.
(B) and **(C)** Chlorophyll fluorescence parameter (1-qP) related to the reduction of Q_A.
(D) and **(E)** PSII yield in the light measured as (Fm'-Fs)/Fm'; wild-type progenitor (dark bars) and *pgrl1* (white bars) lines. Shown are means ± SD (n = 3).

Oxygen Photoreduction in *pgrl1* Is Less Sensitive to Respiratory Inhibitors

Light-dependent O_2 exchange was then measured using a membrane inlet mass spectrometer (MIMS) and [^{18}O]-labeled O_2 (Figure 5). This technique allows measuring O_2 uptake fluxes in the light (Dimon et al., 1988; Beckmann et al., 2009), which may result from different processes, including mitochondrial respiration, photorespiration, or oxygen photoreduction at PSI (Badger, 1985; Peltier and Thibault, 1985). Net O_2 production was mainly unaffected in all conditions tested, except in HL air conditions, where *pgrl1* showed lower activity (Figure 5A). Light-dependent O_2 uptake was higher in the *pgrl1* mutant than in the wild-type line when cells were grown in "air LL" (Figure 5B). To determine the contribution of mitochondrial respiration to the light-dependent O_2 uptake process, we used mitochondrial respiratory inhibitors myxothiazol and SHAM (Figures 5C and 5D). In "HL" grown cells, net O_2 production measured in *pgrl1* was more sensitive to respiratory inhibitors than in its wild-type progenitor (Figure 5C). By contrast, the light-dependent O_2 uptake was much less sensitive to respiratory inhibitors in *pgrl1* than in the wild-type line (Figure 5D), thus indicating that an O_2 uptake process independent of mitochondrial respiration and most likely resulting from O_2 photoreduction (also called the Mehler reactions) was triggered in the mutant.

O_2 photoreduction or Mehler reactions can result from direct interaction of reduced PSI electron acceptors or reduced Fd with molecular O_2, thus producing superoxide and in turn H_2O_2 (Asada, 1999; Rutherford et al., 2012). In cyanobacteria, and possibly in microalgae, a Mehler-like reaction may also result from the action of FLV proteins that use NADPH as an electron donor and produce water (Vicente et al., 2002; Helman et al., 2003). To gain insight into the nature of the O_2 photoreduction mechanism triggered in the *pgrl1* mutant, we first measured extracellular production of H_2O_2 (Figures 6A and 6B). Indeed, wild-type as well as photosynthetic mutant *C. reinhardtii* lines produce H_2O_2 in the extracellular medium during HL exposure (Allorent et al., 2013). This phenomenon occurs when the electron flow capacity is saturated at the level of PSI acceptors, thus triggering O_2 photoreduction. H_2O_2 production was relatively low in most conditions and increased in "air HL" (when compared with "air LL") conditions both in the wild-type and in the mutant lines, the increase being much more pronounced in the mutant (Figure 6B). Immunoblots performed with an antibody recognizing both *C. reinhardtii* FLVA and FLVB proteins showed that both protein amounts are higher in the *pgrl1* mutant than in wild-type progenitor in conditions of high CO_2 (Figure 6C). In air growth conditions, higher FLVB amounts were observed in *pgrl1* in comparison to the wild type, FLVA levels remaining unchanged (Figure 6D). It is concluded from these experiments that the decreased sensitivity of O_2 photoreduction to respiratory inhibitors observed in *pgrl1* (Figure 5D) may result from two effects: (1) an increase in FLVs (Figures 6C and 6D) and likely in FLV-mediated O_2 photoreduction in most conditions; and (2) an additional increase in direct O_2 photoreduction (Mehler reactions) leading to the production of H_2O_2, the latter occurring essentially in air (Figure 6B).

Adaptation Mechanisms Involved in *pgrl1* during a Switch from High to Low CO_2

Adaptation of the *pgrl1* mutant to low CO_2 was then investigated during a switch at HL from high CO_2 to low (air) CO_2 concentration (Figure 7). In conditions of low CO_2, *C. reinhardtii* cells

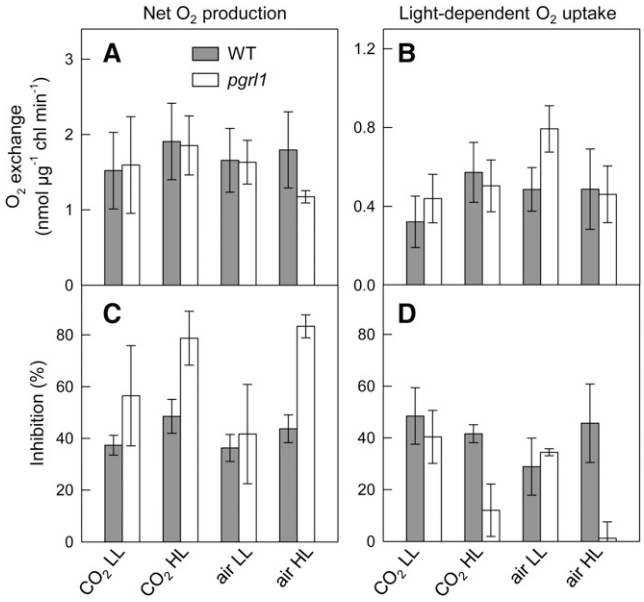

Figure 5. Light-Dependent O_2 Exchange Measured Using a MIMS in Wild-Type and *pgrl1* Cells Grown under Different Light and CO_2 Conditions and Effect of Respiratory Inhibitors.

Cells were grown photoautotrophically under LL (50 µmol photons m^{-2} s^{-1}) or HL (200 µmol photons m^{-2} s^{-1}) in batch cultures in the presence of air or 2% CO_2 in air. O_2 exchange rates were measured using a MIMS in the presence of [^{18}O]-enriched O_2, first during a 5-min dark period and then during a 10-min light period (600 µmol photons m^{-2} s^{-1}).

(A) Net O_2 production in the light.

(B) Light-dependent O_2 uptake.

(C) and **(D)** Inhibition ratios of net O_2 production **(C)** and of light-dependent O_2 uptake **(D)** following incubation of cells with inhibitors of mitochondrial respiration (0.4 mM SHAM and 2 µM myxothiazol). Wild type (dark bars); *pgrl1* (white bars). Shown are means ± SD (n = 3).

induce CCM, therefore increasing the ATP demand of photosynthesis (Fridlyand, 1997; Duanmu et al., 2009; Lucker and Kramer, 2013). We first checked CCM induction by monitoring the increase in carbonic anhydrase activity of intact cells (Supplemental Figure 4A) and accumulation of the low-carbon-inducible protein LCIB (Yamano et al., 2010) (Figure 7A). Abundances of different photosynthetic and respiratory components were then determined by immunoblot analysis (Figure 7A). A transient increase in PGRL1 amounts was observed in the wild-type control (between 2 and 4 h after the switch), indicating an involvement of the PGRL1-mediated CEF to the supply of extra ATP for the CCM. While PSI and PSII amounts, probed by PSAC and PSBD subunits, respectively, increased in the wild type between 4 and 24 h after the switch, almost no change was observed in *pgrl1*. The PSI-to-PSII ratio measured by electrochromic shift (ECS) increased in the wild type, but markedly decreased in *pgrl1* (Figure 7C). Accumulation of LIGHT-HARVESTING COMPLEX STRESS-REGULATED PROTEIN3 (LHCSR3), a light-harvesting protein involved in NPQ and stress response (Peers et al., 2009), occurred 4 h after the switch to low CO_2. Such an increase in LHCSR proteins has been previously reported during *C. reinhardtii* adaptation to low CO_2 (Miura et al., 2004). While LHCSR3 amounts decreased in the wild type at 24 h, a high level remained in *pgrl1*, indicating the persistence of a stress response. Mitochondrial alternative oxidase (AOX) also increased in response to low CO_2 adaptation, but at a later stage, a higher increase being observed in *pgrl1* than in wild-type cells. Note that a lower molecular weight band (presumably corresponding to AOX2) was detected after 6 h and accumulated at 24 h in higher amounts in *prgl1* than in wild-type cells. Amounts of the Fe-superoxide dismutase (FeSOD) and of a subunit of the cytochrome oxidase complex (COXIIb) increased during the switch in a similar manner in both strains. As observed before (Figure 6C; see CO_2 HL conditions), initial FLVA and FLVB amounts were higher in *pgrl1* than in wild-type cells and then decreased in the wild type upon shifting from high to low CO_2 while remaining at a high level in the mutant (Figure 7B). At 24 h, a decrease in both FLVA and FLVB occurred in the mutant, FLVB amounts remaining higher than in the wild type (Figure 7B). Measurements of light-induced O_2 exchange by MIMS showed an increase in the light-dependent O_2 uptake rate in both strains, with the effect more pronounced in *pgrl1* 2 h after the switch (Figure 7D; Supplemental Figure 5). ECS measurements of carotenoids showed that, as expected for a mutant affected in CEF, the partitioning of the proton-motive force between the electrical component ($\Delta\Psi$) and the difference in proton concentration (ΔpH) was constitutively altered in *pgrl1* (Supplemental Figure 6A). Upon transfer to low CO_2, the ΔpH contribution to proton motive force increased significantly in the wild type and remained at a low level in *pgrl1* (Supplemental Figure 6B). An increase of ECS was observed in *pgrl1* (Supplemental Figure 6C), which mirrored the decrease in PSI amounts (Figure 7A), showing that the PSI centers that remain active are capable of turning over faster. Finally, the time-resolved growth rate patterns were analyzed during the transient, showing that both strains reached a similar value ~12 h after the switch (Figure 7E). However, the growth rate took longer to stabilize in *pgrl1* due to the existence of a strong oscillatory regime. We conclude from these data that adaptation of *C. reinhardtii* cells to low CO_2 involves a complex set of mechanisms with different time responses. In the wild type, a fast and transient increase in PGRL1 amounts is followed by an increase in PSI (Figure 7A). In the *pgrl1* the mutant, the absence of PGRL1 increase is compensated for by an upregulation of FLVs (Figures 7B), which is maintained at a higher level than in the wild type, resulting in a higher light-dependent O_2 uptake rate. On a longer time scale, FLV amounts decrease and a different set of mechanisms is triggered, including upregulation of LHCSR3, AOX, and a decrease of the PSI/PSII ratio.

DISCUSSION

We have shown in this study that steady state growth and biomass productivity of the *pgrl1 C. reinhardtii* mutant are comparable to that of the wild-type progenitor line under a wide range of CO_2 concentrations and light intensities. Growth retardation is observed at ambient CO_2 concentrations only when the *pgrl1* mutant is subjected to fluctuating light conditions. This strongly suggests that alternative mechanisms are triggered in the *pgrl1* mutant, efficiently compensating for the ATP deficit resulting from the absence of PGRL1-mediated CEF (Tolleter et al., 2011).

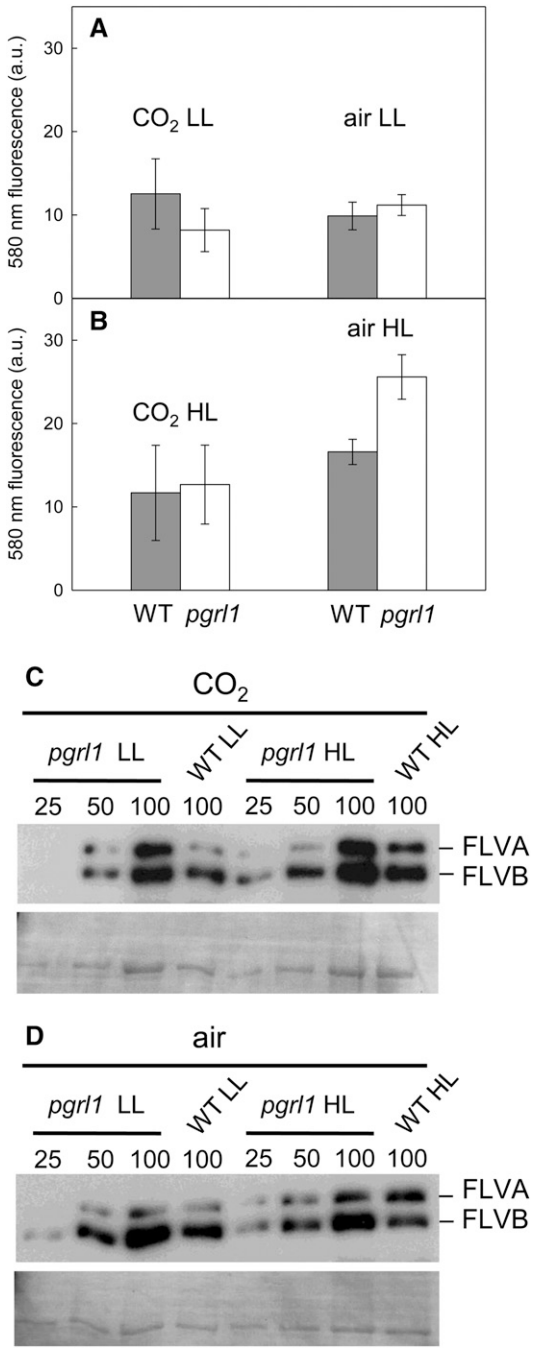

Figure 6. Production of Extracellular Hydrogen Peroxide and Accumulation of FLVs by Wild-Type and *pgrl1* Lines Grown under Different Light and CO_2 Conditions.

(A) and **(B)** Measurements were performed on cells grown photoautotrophically in batch cultures supplied with 2% CO_2 in air or with air in the presence of LL (50 μmol photons m^{-2} s^{-1}) or HL (200 μmol photons m^{-2} s^{-1}). Hydrogen peroxide concentration was assessed in culture medium using Amplex red by measuring fluorescence emission at 580 nm. Wild-type progenitor (dark bars) and *pgrl1* (white bars) lines. Shown are means ± SD (n = 3).

(C) and **(D)** Accumulation of the FLV proteins was determined by immunoblot analysis of wild-type and *pgrl1* lines grown in photobioreactors operated as turbidostats at a constant biomass concentration (≈1.5 × 10^6 cells mL^{-1}). The cultures were grown in 120 μmol photons m^{-2} s^{-1} (LL) or 500 μmol photons m^{-2} s^{-1} (HL) light intensity and in the presence of 2% CO_2 in air **(C)** or in air **(D)**. The FLVB protein has a size of ~60 kD and FLVA shows the faint band at ~70 kD. Fifteen micrograms of total protein as 100% was loaded per lane, and from the *pgrl1* mutant 50 and 25% were loaded as well.

Increased Cooperation with Mitochondrial Respiration

Based on the effect of respiratory inhibitors myxothiazol and SHAM on photosynthesis, we conclude that photosynthetic activity in the *pgrl1* mutant is more dependent on the activity of mitochondrial respiration than in the wild-type line. Such cooperation between photosynthesis and respiration has been widely documented in the past both in higher plants (Krömer and Heldt, 1991; Krömer, 1995) and microalgae (Lemaire et al., 1988). It has been proposed to result from the activity of metabolic shuttles, such as the malate/oxaloacetate valve, which enable the export of reducing power from the chloroplast to the cytosol, and in turn from the cytosol to mitochondria. In *C. reinhardtii*, cooperation with mitochondrial respiration has been proposed to restore photoautotrophic growth in a suppressor strain of a mutant deficient in the plastidial ATPase, by converting reducing power produced in excess into ATP within mitochondria (Lemaire et al., 1988). ATP exchange between cellular compartments is also possible through ATP/ADP translocators or other metabolic shuttles (Hoefnagel et al., 1998). While the mitochondrial ATP/ADP translocator efficiently exports ATP from mitochondria to the cytosol, the DHAP/3-PGA shuttle may be involved in ATP import into the chloroplast (Hoefnagel et al., 1998). However, in contrast with previous works reporting higher COX levels in TAP-grown *pgrl1* cells (Petroutsos et al., 2009; Tolleter et al., 2011), no difference in COX levels was observed between *pgrl1* and wild-type cells during photoautotrophic growth (Figure 7A). While no difference in dark respiration was measured at high CO_2, *pgrl1* showed a 30% higher respiration rate than the wild type after 24 h at low CO_2 (Supplemental Figure 4B). We therefore conclude that the increased dependence of photosynthesis on mitochondrial respiration observed at high CO_2 proceeds via efficient metabolic coupling in the light, but does not result in a sufficient increase in the metabolic pools of respiratory substrates to induce a notable change in dark respiration rates. In spite of a higher dependence of *pgrl1* photosynthesis upon cooperation with mitochondria, we observed under HL a decreased sensitivity of O_2 photoreduction to mitochondrial respiratory inhibitors (Figure 5D). This phenomenon likely results from the activation of O_2 photoreduction mechanisms in the mutant (see discussion below), therefore allowing O_2 uptake to be maintained in the light upon inhibition of respiration by chemicals. We also conclude that the increase in AOX levels observed in the mutant at low CO_2 (Figure 7A), which takes place much later than the stimulation of O_2 photoreduction (Figures 7D), likely reflects a general stress response, as reported in land plants in response to several stress conditions (Millar et al., 2011).

Stimulation of O_2 Photoreduction

Based on measurements of light-dependent O_2 uptake rates and on the effect of mitochondrial respiratory inhibitors, we

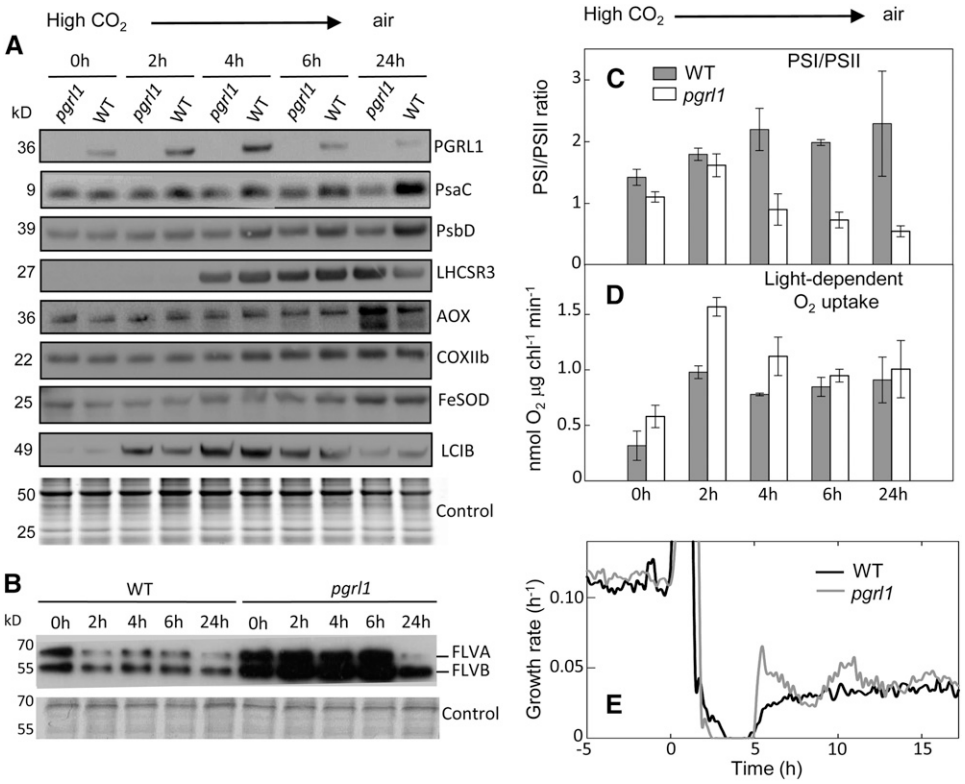

Figure 7. Adaptation of the Photosynthetic Apparatus of *pgrl1* and Wild-Type *C. reinhardtii* Cells to a Switch from High to Low CO_2.

Cells were cultivated autotrophically in photobioreactors operated as turbidostats at a constant biomass concentration (≈1.5 × 10^6 cells mL^{-1}) in the presence of 2% CO_2-enriched air under a light intensity of 500 µmol photons m^{-2} s^{-1}. Upon 48 h stabilization, cultures were shifted to air CO_2 levels (0 h). Samples were taken at 0, 2, 4, 6, and 24 h after the shift in order to perform immunodetection (**[A]** and **[B]**) and functional analysis (**[C]** to **[E]**).
(A) and **(B)** Different antibodies raised against PsaC (PSI), PsbD (PSII), PGRL1, NDA2, AOX1 (AOX), COXIIb (COXII), FeSOD, and FLVs were used to decorate immunoblots. Samples were loaded at equal total proteins amounts based on Coomassie blue staining (Control).
(C) PSI/PSII ratio determined from ECS measurements.
(D) Light-dependent O_2 uptake rates were measured using a MIMS in the presence of [^{18}O]-enriched O_2 as in Figure 5; corresponding O_2 production rates are shown as Supplemental Figure 5.
(E) Growth performances measured as dilution rates used to maintain the culture at a constant biomass concentration; *pgrl1* (gray line) and wild-type control (black line).

concluded that photosynthetic O_2 photoreduction mechanisms are triggered in the *pgrl1* mutant. Such reactions (also called Mehler reactions) may proceed via direct reduction of O_2 by PSI acceptors such as Fd, resulting in the production of reduced O_2 forms (Figure 8) that are detoxified by enzymes of the so-called water-water cycle (Asada, 1999). Since a proton gradient is also formed by electron transfer reactions to O_2, this mechanism participates in the reequilibration of the ATP/NADPH balance through the functioning of pseudocyclic photophosphorylations (Allen, 1975). FLV-mediated O_2 photoreduction may achieve a similar function (Helman et al., 2003; Allahverdiyeva et al., 2011, 2013). Four genes encoding FLV proteins (Flv1, Flv2, Flv3, and Flv4) have been identified in *Synechocystis* PCC6803. While Flv1 and Flv3 are involved in Mehler-like reactions (Helman et al., 2003), likely by forming a heterodimer (Allahverdiyeva et al., 2011), Flv2 and Flv4, the expression of which is triggered at low CO_2 and high light intensity, were proposed to participate in PSII photoprotection (Zhang et al., 2009, 2012). Orthologs to Flv1 and Flv3 are found in green algae and mosses, but not in higher plants (Zhang et al., 2009; Peltier et al., 2010). *C. reinhardtii FLVA* and *FLVB* belong to two clusters containing cyanobacterial Flv1 and Flv2 (for the FlvA cluster) and cyanobacterial Flv3 and Flv4 (for the FlvB cluster) (Zhang et al., 2009; Peltier et al., 2010). The enhanced FLVA and FLVB protein accumulation observed in the *C. reinhardtii pgrl1* mutant compared with its wild-type progenitor, together with the decreased sensitivity of light-dependent O_2 uptake to mitochondrial inhibitors, strongly suggest that FLV proteins are involved in O_2 photoreduction processes downstream of PSI. The absence of FLVA upregulation in *pgrl1* in "air HL" (Figure 7B) might result, as for the decrease in PSI protein amounts observed in the mutant (Figure 7A), from the instability of these proteins under photooxidative stress conditions. As shown in *Synechocystis* cells, FLV-mediated O_2 photoreduction does not result in the production of ROS (Vicente et al., 2002; Helman et al., 2003). The increased H_2O_2 production observed in *pgrl1* in "air HL" may

therefore indicate that FLV-mediated O_2 photoreduction is over-challenged in these conditions, thus resulting in true Mehler reactions producing ROS and H_2O_2 (Figure 8).

State Transition in *pgrl1*

LHCII phosphorylation and a transition from State 1 to State 2 were observed in the *pgrl1* mutant when grown under "air HL" conditions (Figure 2). This phenomenon results from the reduced state of the PQ pool, causing activation of the STT7 kinase that catalyzes phosphorylation of mobile LHCII, which then migrate from PSII (State 1) to PSI (State 2) (Eberhard et al., 2008). Impairments of mitochondrial activity by respiratory inhibitors (Bulté et al., 1990) or by genetic mutations (Cardol et al., 2009) have been shown to induce a highly reduced state of the stromal pools and a transition from State 1 to State 2. A similar phenomenon likely occurs in "air HL"-grown *pgrl1* cells and may be explained by the fact that compensating mechanisms (malate valve/mitochondrial cooperation and O_2 photoreduction) are over-challenged and unable to dissipate the excess of reducing power generated within the chloroplast, therefore resulting in an increase in the reduced state of the PQ pool, phosphorylation of LHCII, and migration of phosphorylated LHCII from PSII to PSI. It is possible that state transition observed in these conditions has a protective role as recently proposed from the study of a *C. reinhardtii* double mutant affected both in qE and state transition (Allorent et al., 2013). The recent finding that CEF and state transition are independent mechanisms (Terashima et al., 2012; Takahashi et al., 2013) might explain how state transition may have a role in the absence of PGRL1-mediated CEF activity.

Control of Linear Electron Flow by the Proton Gradient Generated by CEF

It has been shown that CEF generates a proton gradient that controls linear electron flow at the level of the cytochrome b_6/f complex (Avenson et al., 2005; Joliot and Johnson, 2011), thus protecting PSI from photoinhibition (Suorsa et al., 2012). Under anaerobic conditions, hydrogen production is enhanced in the *pgrl1* mutant due to decreased inhibition of cytochrome b_6/f activity resulting from a restricted proton gradient (Tolleter et al., 2011). In these conditions, protons are used as electron acceptors thanks to the activity of the plastidial [FeFe] hydrogenase. A similar situation likely occurs in aerobic conditions, but in that case O_2 is used as an electron sink, electrons generated in excess at the PSI acceptor side being used to reduce O_2 either in chloroplasts (by direct or FLV-mediated O_2 reduction), or in mitochondria thanks to the export of reducing power by metabolic shuttles.

ATP Requirement of Photosynthesis in Land Plants and Microalgae

Growth and photosynthesis of *pgr5* and *pgrl1 Arabidopsis* mutants were reported to be lower than in the wild-type in plants grown in air (Munekage et al., 2002; DalCorso et al., 2008), the decrease being almost totally suppressed when *pgr5* was grown in air enriched with 2% CO_2 (Munekage et al., 2008). This differs from the phenotype of the *C. reinhardtii pgrl1* mutant described here. Indeed, in liquid cultures, no growth difference was observed between the *C. reinhardtii* mutant and its wild-type progenitor line under steady state growth conditions either at high or at low CO_2 concentration. An explanation to such a difference may be related to the ATP requirement of photosynthesis. In microalgae, the activity of photorespiration is low due to the existence of a CCM. The CCM needs additional energy to function, most likely supplied by ATP (Karlsson et al., 1994; Duanmu et al., 2009). During C_3 photosynthesis, and in the absence of photorespiration (high CO_2 concentration), each CO_2 molecule requires three ATP and two NADPH to be assimilated, corresponding to an ATP/NADPH ratio of 1.5. The ATP demand of CO_2 fixation is increased in conditions of photorespiration (low CO_2), the ATP/NADPH ratio increasing up to 1.62 (Foyer et al., 2012). In microalgae, the CCM would require at least one extra ATP per assimilated CO_2 molecule (Fridlyand, 1997). Therefore, the ATP/NADPH requirement ratio would increase up to a value of two (or even more). PGRL1 amounts increased in the wild type during adaptation to low CO_2, indicating as recently proposed (Lucker and Kramer, 2013), a higher contribution to the increased ATP demand. Increased O_2 photoreduction was also observed in the wild type during adaptation to low CO_2 (Figure 7D), indicating, as previously proposed (Sultemeyer et al., 1993), a contribution of pseudocyclic photophosphorylation to the energy requirement of the CCM. Note that this was not accompanied by upregulation of FLV proteins at low CO_2 (Figure 7B). Therefore, different mechanisms are triggered in *pgrl1* to compensate for the ATP deficiency, including increased cooperation with mitochondrial respiration (Figure 5) and increased O_2 photoreduction associated with the persistence of high FLV protein levels (Figures 7B and 7D). In this context, the absence of FLV-mediated O_2 photoreduction in land plants and/or the existence of less efficient cooperation with mitochondria would explain the defect in growth observed in *Arabidopsis pgr5* (Munekage et al., 2002, 2008) or *pgrl1* mutants (DalCorso et al., 2008). Differences in growth phenotypes observed under fluctuating light between land plants and algal mutants may result from similar causes. Indeed, while the *Arabidopsis pgr5* mutant does not grow under fluctuating light (Tikkanen et al., 2010), growth of the *C. reinhardtii pgrl1* mutant is only slightly affected compared with that of the wild-type progenitor line (Figure 3). The growth decrease observed in the *C. reinhardtii pgrl1* mutant does not seem to result from a direct inhibitory effect, but rather from the incapacity of the mutant to take advantage of the HL pulse (Figures 3I and 3J). Additional fluctuating light experiments on the *Arabidopsis pgrl1* mutant and/or on the recently isolated *C. reinhardtii pgr5* mutant (Johnson et al., 2014) will be needed to determine whether such phenotypic differences are related to the target gene (*pgrl1 v pgr5*) or to the recipient species (*C. reinhardtii v Arabidopsis*).

Proposed Cascade of Events Occurring in *pgrl1* in Response to Increased ATP Demand

Based on our data, we propose a scenario in which different mechanisms would be sequentially triggered in the *pgrl1* mutant in response to increased ATP demand to reequilibrate the

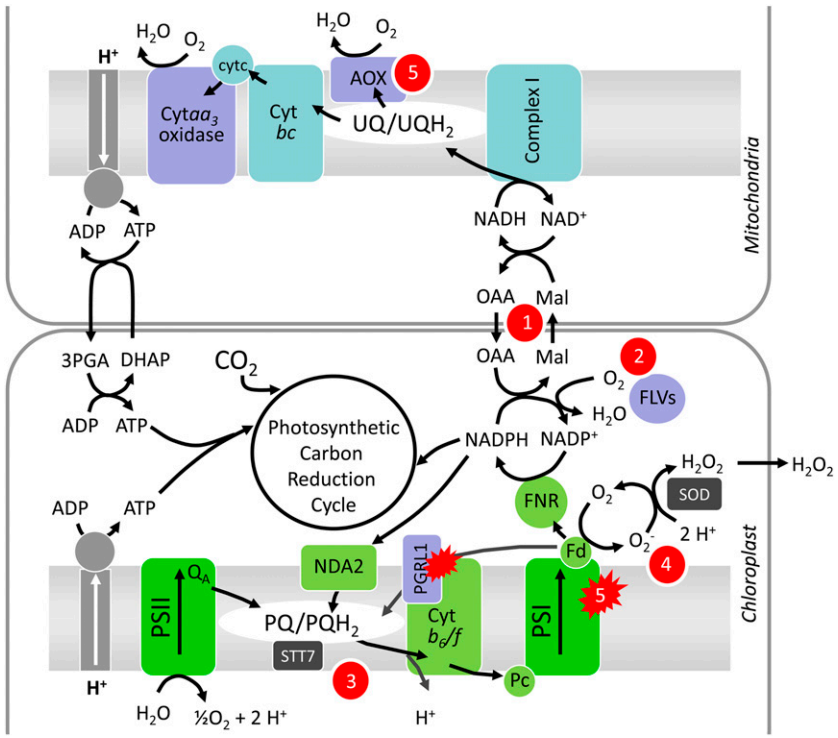

Figure 8. Schematic Diagram of Electron Transfer Reactions Involved in Oxygenic Photosynthesis in Chloroplasts and Mitochondria and Their Regulation in the Absence of PGRL1-Mediated CEF.

During reactions of linear electron transport, reducing equivalents generated at PSII are sequentially transferred to plastoquinones (PQ/PQH_2), cytochrome (Cyt) b_6/f complex, plastocyanin (Pc), PSI, Fd, and to ferredoxin $NADP^+$ reductase (FNR). A pathway of cyclic electron flow around PSI is mediated by PGRL1 and another one by NDA2. In the absence of PGRL1, the deficiency in ATP is compensated for by different mechanisms, sequentially triggered depending on the intensity of the ATP demand. (1) A first compensation mechanism operates via cooperation with mitochondrial respiration, likely involving the oxaloacetate/malate shuttle (or malate valve), which allows export of reducing power from the chloroplast to the cytosol and from the cytosol to mitochondria. In mitochondria, reducing power is converted by the electron transport chain into ATP, which can reenter the chloroplast via ATP translocators. (2) Oxygen photoreduction may occur at the level of NADPH thanks to the action of FLVA and FLVB proteins, which accumulate to higher amounts in *pgrl1* and would allow ATP biosynthesis through pseudocyclic photophosphorylation. (3) When mechanisms (1) and (2) are overengaged, the PQ pool becomes more reduced, and the STT7 kinase is activated, thus inducing LHCII phosphorylation and transition from State 1 to State 2 in *pgrl1*. (4) Finally overreduction of PSI acceptors would trigger true Mehler reactions through direct O_2 photoreduction via reduced Fd, thus producing H_2O_2. (5) Accumulation of ROS would then increase AOX and decrease PSI protein amounts, thus decreasing the PSI/PSII ratio.

ATP/NADPH imbalance resulting from the absence of PGRL1-mediated CEF (Figure 8). When the ATP demand is relatively low, increased coupling with mitochondria and increased FLV-mediated O_2 photoreduction would allow the dissipation of excess reducing power and supply sufficient ATP, resulting in reequilibration of the ATP/NADPH ratio. However, these mechanisms would not be able to dissipate excess electrons and compensate for the ATP deficit as the ATP demand increases ("air HL"). As a consequence, the redox state of the stromal NADPH pool would increase, thus resulting in increased leakage of electrons to O_2 at PSI and in a more reduced PQ pool, which would in turn activate the STT7 kinase responsible for LHCII phosphorylation and trigger transition to State 2. Increased direct O_2 photoreduction would again reequilibrate the ATP/NADPH ratio, but this would be accompanied by an enhanced production of H_2O_2 therefore resulting in PSI photodamage and a decrease of the PSI/PSII ratio.

We conclude from this study that the CO_2 assimilation machinery is capable of great flexibility and adaptation. The deficiency of PGRL1-mediated CEF can be compensated for at steady state by a set of mechanisms, resulting in similar growth performance and biomass productivity. However, these compensation mechanisms are not perfect. First, they operate on a longer time scale, causing the mutant to exhibit a growth delay during a high light transient or oscillatory growth upon adaptation to low CO_2. Second, they have limited activity and, when overcome, may be accompanied by the production of ROS, which are detoxified to a certain extent, but may induce a decrease in PSI and an impairment of photosynthetic capacity. PGRL1-mediated CEF may therefore have been selected for during evolution as a mechanism allowing rapid adaptation of the photosynthetic electron transport chain in response to sudden changes in the environment.

METHODS

Strains and Growth Conditions

The *Chlamydomonas reinhardtii* wild-type strain CC124 (*mt⁻ nit1 nit2*), progenitor of the *pgrl1* mutant, and the *pgrl1*-ko mutant (Tolleter et al., 2011) were grown at 25°C under continuous illumination on minimal culture medium (Harris, 1989). Batch cultures were grown on a rotary shaker in Erlenmeyer flasks (100 mL) placed in a thermoregulated (25°C) incubator (Multitron; Infors) under continuous illumination (50 or 200 μmol photons m^{-2} s^{-1}) in the presence of air or 2% CO_2-enriched air. For continuous photoautotrophic growth experiment, cells were cultured in four autoclavable 1-liter photobioreactors (BIOSTAT Aplus; Sartorius Stedim Biotech) equipped with a biomass probe (Excell probe, Exner; measuring OD_{880} with a 2-cm light path) and operated as turbidostats. A regulation system allowed the maintenance of cultures at a constant OD_{880} by injection of fresh medium (Stepdos FEM03TT18RC; KNF). The pH (Easyferm K160; Hamilton) was maintained at a constant value (pH 7.0) by injection of 0.2 N KOH or 0.2 N HCl using the BIOSTAT module. The cultures were stirred using a marine propeller (250 rpm). The gas flow rate was adjusted to 0.5 liters min^{-1}. The air + 2% CO_2 gas mixture was generated using two mass flow meters (EL flow; Bronkhorst). Light was supplied by eight fluorescent tubes (Osram Dulux L 18 W) placed radially around the photobioreactor to reach light intensities (measured at the surface of the photobioreactor) up to 1200 μmol photons m^{-2} s^{-1}. Growth rates (d^{-1}) were calculated by dividing the daily dilution volume by the photobioreactor volume (1 liter). In some experiments, cells were grown in fluctuating illumination by continuously switching from 5-min LL (50 μmol photon m^{-2} s^{-1}) periods to 1-min HL periods (800 μmol photon m^{-2} s^{-1}).

Chlorophyll fluorescence measurements were performed using a Dual Pulse Amplitude Modulated Fluorometer (DUAL-PAM-100; Walz). For *Fv/Fm* and NPQ measurements, samples were placed into a cuvette under constant stirring at room temperature (23°C) and dark adapted (30 min). NPQ measurements were performed during a transition from darkness to 800 μmol photons m^{-2} s^{-1} light (Peers et al., 2009). For ETR measurements, cells were not dark-adapted to avoid inactivation of enzymes of the Calvin cycle. Upon sampling, $NaHCO_3$ (5 mM final concentration) and MOPS buffer (pH 7.5, 1 mM final concentration) were added, and actinic light was increased stepwise (every 2 min) from 50 to 500 μmol photons m^{-2} s^{-1}. Saturating flashes (10,000 μmol photons m^{-2} s^{-1}, 200-ms duration) were supplied at different time points to determine PSII yield, 1-qP, NPQ (Schreiber et al., 1986; Klüghammer and Schreiber, 2008). ETR was calculated as described previously (Rumeau et al., 2005).

Electrochromic shifts of carotenoids were measured as absorbance changes at 520 nm using a JTS10 spectrophotometer as described by Tolleter et al. (2011). PSI/PSII stoichiometries were evaluated from the signal induced by a saturating single turnover flash in the absence or in the presence of PSII inhibitors hydroxylamine and DCMU at final concentrations of 1 mM and 10 μM, respectively. Continuous illumination was 1000 μmol photons m^{-2} s^{-1}.

Immunoblot Analysis

Whole-cell extracts were rapidly harvested and frozen from photobioreactor cultures. Proteins were extracted and separated under denaturing conditions (10% PAGE Bis-Tris SDS-MOPS). Antiphosphothreonine antibody (Zymed) was used to reveal phosphorylated proteins. Representative subunits of photosynthetic complexes were used to decorate immunoblots: anti-PsaC (PSI), anti-PsbD (PSII), anti-cytf (*cytb$_6$f*), anti-AOX1 (AOX), anti-COXIIb (COXII), and anti-FeSOD, all purchased from Agrisera. Horseradish peroxidase chemiluminescent substrate was used to reveal the antibody signal using the GBOX imaging system (Syngene). The LCIB antibody was kindly supplied by H. Fukuzawa (Yamano et al., 2010). Anti-PGRL1 and anti-NDA2 were previously described by Tolleter et al. (2011) and Desplats et al. (2009), respectively. For FLV immunoblot analysis, total proteins were separated in SDS-PAGE (14% polyacrylamide, without urea), electroblotted to a polyvinylidene difluoride membrane (Millipore), and blocked with 5% blotting grade blocker (Bio-Rad). FLVB was detected using a purified rabbit antibody prepared against a peptide antigen mix (CKVVIAESYGGRDEP and CARKKAAMSGEVAKA) conjugated with keyhole limpet hemocyanin. Due to the high homology, this antibody recognizes also FLVA protein. As a secondary antibody, anti-rabbit horseradish peroxidase was used 1:10,000 and visualized with ECL.

77K Chlorophyll Fluorescence Spectra

Low-temperature fluorescence spectra were measured on whole cells at 77K using a SAFAS Xenius optical fiber fluorescence spectrophotometer. Light-adapted cell suspension (1.5 mL at ~1.5 × 10^6 cells mL^{-1}), cultivated in different conditions of illumination and CO_2 supply, was frozen in a liquid nitrogen bath cryostat (Optisat DN; Oxford Instruments). The excitation wavelength was 440 nm, and excitation and emission slits were 10 and 5 nm, respectively.

Measurement of O_2 Exchange Using a MIMS

O_2 exchanges were measured in the presence of [^{18}O]-enriched O_2 using a water-jacketed, thermoregulated (25°C) reaction vessel coupled to a mass spectrometer (model Prima δB; Thermo Electron) through a membrane inlet system (Tolleter et al., 2011). The cell suspension (1.5 mL) was placed in the reaction vessel and bicarbonate (5 mM final concentration) was added to reach a saturating CO_2 concentration. One hundred microliters of [^{18}O]-enriched O_2 (99% $^{18}O_2$ isotope content; Euriso-Top) was bubbled at the top of the suspension just before vessel closure and gas exchange measurements. O_2 exchanges were measured during a 5-min period in the dark, then the suspension was illuminated at 600 μmol photons m^{-2} s^{-1} for 10 min. Isotopic O_2 species [$^{18}O^{18}O$] (m/e = 36), [$^{18}O^{16}O$] (m/e = 34), and [$^{16}O^{16}O$] (m/e = 32) were monitored, and O_2 exchange rates were determined as described previously (Cournac et al., 2002). When indicated, mitochondrial respiratory inhibitors myxothiazol and SHAM were added 15 min before starting measurements at final concentrations of 2 μM and 0.4 mM, respectively.

Production of Extracellular H_2O_2

Extracellular H_2O_2 was detected as described (Allorent et al., 2013) using the Amplex Red reagent (Invitrogen). Cells were centrifuged once and supernatant was incubated for 30 min in the dark in the presence of the Amplex Red reagent (2.5 μM final concentration) and horseradish peroxidase (0.025 units mL^{-1}; Sigma-Aldrich) forming the fluorescent resofurin product. Fluorescence emission at 580 nm (excitation 540 nm) was measured on a SAFAS Xenius fluorescence spectrophotometer.

Accession Numbers

Sequence data from this article can be found in the GenBank/EMBL databases under the following accession numbers: AOX1 (EMBL EDP02600.1), AOX2 (EMBL EDP06011.1), FLVA (EMBL EDP03485.1), FLVB (EMBL EDO98775.1), LCIB (EMBL ABG38184.1), LHCSR3 (EMBL EDP01087.1), NDA2 (EMBL EDO96450.1), PGRL1 (GenBank XP_001700905), PsaC (EMBL AAB17714.1), and PsbD (EMBL P06007.1).

Supplemental Data

The following materials are available in the online version of this article.

Supplemental Figure 1. Photosynthetic Activity of *C. reinhardtii* Wild-Type and *pgrl1* Mutant Lines Measured by Chlorophyll Fluorescence.

Supplemental Figure 2. ETR Capacities and 77K Chlorophyll Fluorescence Measured in Wild-Type and *pgrl1* during Transients from Moderate to High Light Performed under Two Different CO_2 Concentrations.

Supplemental Figure 3. Accumulation of NDA2 and PGRL1 Proteins in Wild-Type and *pgrl1 C. reinhardtii* Lines Grown under Different Environmental Conditions.

Supplemental Figure 4. Effect of a High-to-Low (air) CO_2 Concentration Switch on Carbonic Anhydrase Activity and Mitochondrial Respiration Measured on Intact Cells.

Supplemental Figure 5. Light-Dependent O_2 Exchange Measured in Wild-Type and *pgrl1* Cells Shifted from High CO_2 to Low CO_2 (Air).

Supplemental Figure 6. Electrochromic Shift (ECS) and Proton Concentration (ΔpH) in *pgrl1* and Wild-Type *C. reinhardtii* Cells to a Switch from High to Low CO_2.

ACKNOWLEDGMENTS

This work was supported by the French "Agence Nationale pour la Recherche" (ALGOMICS and ALGOH2 projects) and by the CNRS-JST joined program "Structure and Function of Biomolecules." Support was also provided by the HélioBiotec platform, funded by the European Union (European Regional Development Fund), the Région Provence Alpes Côte d'Azur, the French Ministry of Research, and the "Commissariat à l'Energie Atomique et aux Energies Alternatives." Y.A. and M.J. acknowledge the Academy of Finland (project number 271832). We thank H. Fukuzawa (Kyoto University, Japan) for the generous gift of the LCIB antibody.

AUTHOR CONTRIBUTIONS

J.P., D.T., K.-V.D., and G.P. designed the research. K.-V.D., J.P., D.T., M.J., S.C., P.C., P.A., P.R., X.J., and J.A. performed the research. K.-V.D., J.P., D.T., M.J., Y.A., X.J., J.A., and G.P. analyzed the data. G.P. wrote the article.

Received April 8, 2014; revised May 21, 2014; accepted June 13, 2014; published July 2, 2014.

REFERENCES

Allahverdiyeva, Y., Ermakova, M., Eisenhut, M., Zhang, P., Richaud, P., Hagemann, M., Cournac, L., and Aro, E.M. (2011). Interplay between flavodiiron proteins and photorespiration in *Synechocystis* sp. PCC 6803. J. Biol. Chem. **286:** 24007–24014.

Allahverdiyeva, Y., Mustila, H., Ermakova, M., Bersanini, L., Richaud, P., Ajlani, G., Battchikova, N., Cournac, L., and Aro, E.M. (2013). Flavodiiron proteins Flv1 and Flv3 enable cyanobacterial growth and photosynthesis under fluctuating light. Proc. Natl. Acad. Sci. USA **110:** 4111–4116.

Allen, J.F. (1975). Oxygen reduction and optimum production of ATP in photosynthesis. Nature **256:** 599–600.

Allorent, G., et al. (2013). A dual strategy to cope with high light in *Chlamydomonas reinhardtii.* Plant Cell **25:** 545–557.

Asada, K. (1999). The water-water cycle in chloroplasts: Scavenging of active oxygens and dissipation of excess photons. Annu. Rev. Plant Physiol. Plant Mol. Biol. **50:** 601–639.

Avenson, T.J., Cruz, J.A., Kanazawa, A., and Kramer, D.M. (2005). Regulating the proton budget of higher plant photosynthesis. Proc. Natl. Acad. Sci. USA **102:** 9709–9713.

Badger, M.R. (1985). Photosynthetic oxygen-exchange. Annu. Rev. Plant Physiol. Plant Mol. Biol. **36:** 27–53.

Beckmann, K., Messinger, J., Badger, M.R., Wydrzynski, T., and Hillier, W. (2009). On-line mass spectrometry: membrane inlet sampling. Photosynth. Res. **102:** 511–522.

Bulté, L., Gans, P., Rebéillé, F., and Wollman, F.-A. (1990). ATP control on state transitions *in vivo* in *Chlamydomonas reinhardtii.* Biochim. Biophys. Acta **1020:** 72–80.

Cardol, P., Alric, J., Girard-Bascou, J., Franck, F., Wollman, F.A., and Finazzi, G. (2009). Impaired respiration discloses the physiological significance of state transitions in *Chlamydomonas.* Proc. Natl. Acad. Sci. USA **106:** 15979–15984.

Cournac, L., Latouche, G., Cerovic, Z., Redding, K., Ravenel, J., and Peltier, G. (2002). *In vivo* interactions between photosynthesis, mitorespiration, and chlororespiration in *Chlamydomonas reinhardtii.* Plant Physiol. **129:** 1921–1928.

DalCorso, G., Pesaresi, P., Masiero, S., Aseeva, E., Schünemann, D., Finazzi, G., Joliot, P., Barbato, R., and Leister, D. (2008). A complex containing PGRL1 and PGR5 is involved in the switch between linear and cyclic electron flow in *Arabidopsis.* Cell **132:** 273–285.

Delepelaire, P., and Wollman, F.A. (1985). Correlations between fluorescence and phosphorylation changes in thylakoid membranes of *Chlamydomonas reinhardtii in vivo* - A kinetic analysis. Biochim. Biophys. Acta **809:** 277–283.

Desplats, C., Mus, F., Cuiné, S., Billon, E., Cournac, L., and Peltier, G. (2009). Characterization of Nda2, a plastoquinone-reducing type II NAD(P)H dehydrogenase in *Chlamydomonas* chloroplasts. J. Biol. Chem. **284:** 4148–4157.

Dimon, B., Gans, P., and Peltier, G. (1988). Mass-spectrometric measurement of photosynthetic and respiratory oxygen-exchange. Methods Enzymol. **167:** 686–691.

Duanmu, D., Miller, A.R., Horken, K.M., Weeks, D.P., and Spalding, M.H. (2009). Knockdown of limiting-CO_2-induced gene HLA3 decreases HCO_3^- transport and photosynthetic Ci affinity in *Chlamydomonas reinhardtii.* Proc. Natl. Acad. Sci. USA **106:** 5990–5995.

Eberhard, S., Finazzi, G., and Wollman, F.A. (2008). The dynamics of photosynthesis. Annu. Rev. Genet. **42:** 463–515.

Fleischmann, M.M., Ravanel, S., Delosme, R., Olive, J., Zito, F., Wollman, F.-A., and Rochaix, J.-D. (1999). Isolation and characterization of photoautotrophic mutants of *Chlamydomonas reinhardtii* deficient in state transition. J. Biol. Chem. **274:** 30987–30994.

Foyer, C.H., Neukermans, J., Queval, G., Noctor, G., and Harbinson, J. (2012). Photosynthetic control of electron transport and the regulation of gene expression. J. Exp. Bot. **63:** 1637–1661.

Fridlyand, L.E. (1997). Models of CO_2 concentrating mechanisms in microalgae taking into account cell and chloroplast structure. Biosystems **44:** 41–57.

Harris, E.H. (1989). The *Chlamydomonas* Sourcebook: A Comprehensive Guide to Biology and Laboratory Use. (San Diego, CA: Academic Press).

Helman, Y., Tchernov, D., Reinhold, L., Shibata, M., Ogawa, T., Schwarz, R., Ohad, I., and Kaplan, A. (2003). Genes encoding A-type flavoproteins are essential for photoreduction of O_2 in cyanobacteria. Curr. Biol. **13:** 230–235.

Hertle, A.P., Blunder, T., Wunder, T., Pesaresi, P., Pribil, M., Armbruster, U., and Leister, D. (2013). PGRL1 is the elusive ferredoxin-plastoquinone reductase in photosynthetic cyclic electron flow. Mol. Cell **49:** 511–523.

Hoefnagel, M.H.N., Atkin, O.K., and Wiskich, J.T. (1998). Interdependence between chloroplasts and mitochondria in the light and the dark. Biochim. Biophys. Acta **1366:** 235–255.

Iwai, M., Takizawa, K., Tokutsu, R., Okamuro, A., Takahashi, Y., and Minagawa, J. (2010). Isolation of the elusive supercomplex that drives cyclic electron flow in photosynthesis. Nature **464:** 1210–1213.

Jans, F., Mignolet, E., Houyoux, P.A., Cardol, P., Ghysels, B., Cuiné, S., Cournac, L., Peltier, G., Remacle, C., and Franck, F. (2008). A type II NAD(P)H dehydrogenase mediates light-independent plastoquinone reduction in the chloroplast of *Chlamydomonas.* Proc. Natl. Acad. Sci. USA **105:** 20546–20551.

Joët, T., Cournac, L., Horvath, E.M., Medgyesy, P., and Peltier, G. (2001). Increased sensitivity of photosynthesis to antimycin A induced by inactivation of the chloroplast *ndhB* gene. Evidence for a participation of the NADH-dehydrogenase complex to cyclic electron flow around photosystem I. Plant Physiol. **125:** 1919–1929.

Johnson, X., et al. (2014). Proton Gradient Regulation 5-mediated cyclic electron flow under ATP- or redox-limited conditions: a study of Δ*ATPase pgr5* and Δ*rbcL pgr5* mutants in *Chlamydomonas reinhardtii.* Plant Physiol. **165:** 438–452.

Joliot, P., and Johnson, G.N. (2011). Regulation of cyclic and linear electron flow in higher plants. Proc. Natl. Acad. Sci. USA **108:** 13317–13322.

Karlsson, J., Ramazanov, Z., Hiltonen, T., Gardestrom, P., and Samuelsson, G. (1994). Effect of vanadate on photosynthesis and the ATP/ADP ratio in low-CO_2-adapted *Chlamydomonas reinhardtii* cells. Planta **192:** 46–51.

Klüghammer, C., and Schreiber, U. (2008). Saturation pulse method for assessment of energy conversion in PS I. PAM Application Notes **1:** 11–14.

Kramer, D.M., and Evans, J.R. (2011). The importance of energy balance in improving photosynthetic productivity. Plant Physiol. **155:** 70–78.

Krömer, S. (1995). Respiration during photosynthesis. Annu. Rev. Plant Physiol. Plant Mol. Biol. **46:** 45–70.

Krömer, S., and Heldt, H.W. (1991). On the role of mitochondrial oxidative phosphorylation in photosynthesis metabolism as studied by the effect of oligomycin on photosynthesis in protoplasts and leaves of barley (*Hordeum vulgare*). Plant Physiol. **95:** 1270–1276.

Lemaire, C., Wollman, F.A., and Bennoun, P. (1988). Restoration of phototrophic growth in a mutant of *Chlamydomonas reinhardtii* in which the chloroplast *atpB* gene of the ATP synthase has a deletion: an example of mitochondria-dependent photosynthesis. Proc. Natl. Acad. Sci. USA **85:** 1344–1348.

Lucker, B., and Kramer, D.M. (2013). Regulation of cyclic electron flow in *Chlamydomonas reinhardtii* under fluctuating carbon availability. Photosynth. Res. **117:** 449–459.

Miura, K., Yamano, T., Yoshioka, S., Kohinata, T., Inoue, Y., Taniguchi, F., Asamizu, E., Nakamura, Y., Tabata, S., Yamato, K.T., Ohyama, K., and Fukuzawa, H. (2004). Expression profiling-based identification of CO_2-responsive genes regulated by CCM1 controlling a carbon-concentrating mechanism in *Chlamydomonas reinhardtii.* Plant Physiol. **135:** 1595–1607.

Millar, A.H., Whelan, J., Soole, K.L., and Day, D.A. (2011). Organization and regulation of mitochondrial respiration in plants. Annu. Rev. Plant Biol. **62:** 79–104.

Munekage, Y., Hojo, M., Meurer, J., Endo, T., Tasaka, M., and Shikanai, T. (2002). PGR5 is involved in cyclic electron flow around photosystem I and is essential for photoprotection in *Arabidopsis.* Cell **110:** 361–371.

Munekage, Y., Hashimoto, M., Miyake, C., Tomizawa, K., Endo, T., Tasaka, M., and Shikanai, T. (2004). Cyclic electron flow around photosystem I is essential for photosynthesis. Nature **429:** 579–582.

Munekage, Y.N., Genty, B., and Peltier, G. (2008). Effect of PGR5 impairment on photosynthesis and growth in *Arabidopsis thaliana.* Plant Cell Physiol. **49:** 1688–1698.

Niyogi, K.K. (2000). Safety valves for photosynthesis. Curr. Opin. Plant Biol. **3:** 455–460.

Osmond, C.B. (1981). Photorespiration and photoinhibition. Some implications for the energetics of photosynthesis. Biochim. Biophys. Acta **639:** 77–98.

Peers, G., Truong, T.B., Ostendorf, E., Busch, A., Elrad, D., Grossman, A.R., Hippler, M., and Niyogi, K.K. (2009). An ancient light-harvesting protein is critical for the regulation of algal photosynthesis. Nature **462:** 518–521.

Peltier, G., and Thibault, P. (1985). Oxygen uptake in the light in *Chlamydomonas*. Evidence for persistent mitochondrial respiration. Plant Physiol. **79:** 225–230.

Peltier, G., Tolleter, D., Billon, E., and Cournac, L. (2010). Auxiliary electron transport pathways in chloroplasts of microalgae. Photosynth. Res. **106:** 19–31.

Petroutsos, D., Terauchi, A.M., Busch, A., Hirschmann, I., Merchant, S.S., Finazzi, G., and Hippler, M. (2009). PGRL1 participates in iron-induced remodeling of the photosynthetic apparatus and in energy metabolism in *Chlamydomonas reinhardtii.* J. Biol. Chem. **284:** 32770–32781.

Ravenel, J., Peltier, G., and Havaux, M. (1994). The cyclic electron pathways around photosystem-I in *Chlamydomonas reinhardtii* as determined *in vivo* by photoacoustic measurements of energy storage. Planta **193:** 251–259.

Rumeau, D., Bécuwe-Linka, N., Beyly, A., Louwagie, M., Garin, J., and Peltier, G. (2005). New subunits NDH-M, -N, and -O, encoded by nuclear genes, are essential for plastid Ndh complex functioning in higher plants. Plant Cell **17:** 219–232.

Rutherford, A.W., Osyczka, A., and Rappaport, F. (2012). Back-reactions, short-circuits, leaks and other energy wasteful reactions in biological electron transfer: redox tuning to survive life in $O_{(2)}$. FEBS Lett. **586:** 603–616.

Scheibe, R. (2004). Malate valves to balance cellular energy supply. Physiol. Plant. **120:** 21–26.

Schreiber, U., Schliwa, U., and Bilger, W. (1986). Continuous recording of photochemical and non-photochemical chlorophyll fluorescence quenching with a new type of modulation fluorometer. Photosynth. Res. **10:** 51–62.

Shen, W., Wei, Y., Dauk, M., Tan, Y., Taylor, D.C., Selvaraj, G., and Zou, J. (2006). Involvement of a glycerol-3-phosphate dehydrogenase in modulating the NADH/NAD^+ ratio provides evidence of a mitochondrial glycerol-3-phosphate shuttle in *Arabidopsis.* Plant Cell **18:** 422–441.

Sultemeyer, D., Biehler, K., and Fock, H.P. (1993). Evidence for the contribution of pseudocyclic photophosphorylation to the energy requirement of the mechanism for concentrating inorganic carbon in *Chlamydomonas.* Planta **189:** 235–242.

Suorsa, M., Järvi, S., Grieco, M., Nurmi, M., Pietrzykowska, M., Rantala, M., Kangasjärvi, S., Paakkarinen, V., Tikkanen, M., Jansson, S., and Aro, E.-M. (2012). PROTON GRADIENT REGULATION5 is essential for proper acclimation of *Arabidopsis* photosystem I to naturally and artificially fluctuating light conditions. Plant Cell **24:** 2934–2948.

Takahashi, H., Clowez, S., Wollman, F.-A., Vallon, O., and Rappaport, F. (2013). Cyclic electron flow is redox-controlled but independent of state transition. Nat. Commun. **4:** 1954.

Terashima, M., Petroutsos, D., Hüdig, M., Tolstygina, I., Trompelt, K., Gäbelein, P., Fufezan, C., Kudla, J., Weinl, S., Finazzi, G., and Hippler, M. (2012). Calcium-dependent regulation of cyclic photosynthetic electron transfer by a CAS, ANR1, and PGRL1 complex. Proc. Natl. Acad. Sci. USA **109:** 17717–17722.

Tikkanen, M., Grieco, M., Kangasjärvi, S., and Aro, E.M. (2010). Thylakoid protein phosphorylation in higher plant chloroplasts optimizes electron transfer under fluctuating light. Plant Physiol. **152:** 723–735.

Tolleter, D., et al. (2011). Control of hydrogen photoproduction by the proton gradient generated by cyclic electron flow in *Chlamydomonas reinhardtii.* Plant Cell **23:** 2619–2630.

Vicente, J.B., Gomes, C.M., Wasserfallen, A., and Teixeira, M. (2002). Module fusion in an A-type flavoprotein from the cyanobacterium *Synechocystis* condenses a multiple-component pathway in a single polypeptide chain. Biochem. Biophys. Res. Commun. **294:** 82–87.

Wollman, F.A., and Delepelaire, P. (1984). Correlation between changes in light energy distribution and changes in thylakoid membrane polypeptide phosphorylation in *Chlamydomonas reinhardtii.* J. Cell Biol. **98:** 1–7.

Yamano, T., Tsujikawa, T., Hatano, K., Ozawa, S., Takahashi, Y., and Fukuzawa, H. (2010). Light and low-CO_2-dependent LCIB-LCIC complex localization in the chloroplast supports the carbon-concentrating mechanism in *Chlamydomonas reinhardtii*. Plant Cell Physiol. **51:** 1453–1468.

Zhang, P., Allahverdiyeva, Y., Eisenhut, M., and Aro, E.-M. (2009). Flavodiiron proteins in oxygenic photosynthetic organisms: photoprotection of photosystem II by Flv2 and Flv4 in *Synechocystis* sp. PCC 6803. PLoS ONE **4:** e5331.

Zhang, P., Eisenhut, M., Brandt, A.M., Carmel, D., Silén, H.M., Vass, I., Allahverdiyeva, Y., Salminen, T.A., and Aro, E.M. (2012). Operon flv4-flv2 provides cyanobacterial photosystem II with flexibility of electron transfer. Plant Cell **24:** 1952–1971.